Journal of Nanophotonics

Nanophotonics.SPIEDigitalLibrary.org

Light refocusing with up-scalable resonant waveguide gratings in confocal prolate spheroid arrangements

Giorgio Quaranta
Guillaume Basset
Zdenek Benes
Olivier J. F. Martin
Benjamin Gallinet

SPIE.

Giorgio Quaranta, Guillaume Basset, Zdenek Benes, Olivier J. F. Martin, Benjamin Gallinet, "Light refocusing with up-scalable resonant waveguide gratings in confocal prolate spheroid arrangements," *J. Nanophoton.* **12**(1), 016004 (2018), doi: 10.1117/1.JNP.12.016004.

Light refocusing with up-scalable resonant waveguide gratings in confocal prolate spheroid arrangements

Giorgio Quaranta,[a,b] Guillaume Basset,[a] Zdenek Benes,[c] Olivier J. F. Martin,[b] and Benjamin Gallinet[a,*]

[a]Swiss Center of Electronics and Microtechnology (CSEM S.A.), Muttenz, Switzerland
[b]Swiss Federal Institute of Technology (EPFL), Nanophotonics and Metrology Laboratory (NAM), Lausanne, Switzerland
[c]Swiss Federal Institute of Technology (EPFL), Center of MicroNanoTechnology (CMI), Lausanne, Switzerland

Abstract. Resonant waveguide gratings (RWGs) are thin-film structures, where coupled modes interfere with the diffracted incoming wave and produce strong angular and spectral filtering. The combination of two finite-length and impedance matched RWGs allows the creation of a passive beam steering element, which is compatible with up-scalable fabrication processes. Here, we propose a design method to create large patterns of such elements able to filter, steer, and focus the light from one point source to another. The method is based on ellipsoidal mirrors to choose a system of confocal prolate spheroids where the two focal points are the source point and observation point, respectively. It allows finding the proper orientation and position of each RWG element of the pattern, such that the phase is constructively preserved at the observation point. The design techniques presented here could be implemented in a variety of systems, where large-scale patterns are needed, such as optical security, multifocal or monochromatic lenses, biosensors, and see-through optical combiners for near-eye displays. [DOI: 10.1117/1.JNP.12.016004]

Keywords: light refocusing; up-scalable fabrication; resonant waveguide grating; coupled mode resonance; confocal prolate spheroids; ellipsoidal mirror.

Paper 17167 received Oct. 26, 2017; accepted for publication Jan. 4, 2018; published online Jan. 25, 2018.

1 Introduction

Resonant waveguide gratings (RWGs)[1] are structures of high interest used in a variety of applications such as filters,[2] biochemical sensors,[3] light absorbers,[4] security devices,[5] and grating couplers.[6,7] These resonances were first observed by Wood[8] in the form of anomalous diffraction phenomena in grating structures. Hessel and Oliver[9] started to differentiate anomalous diffractions in two types: the Rayleigh type, which is the classical Wood's anomaly, and the resonance type. The resonance anomalies in the form of coupled mode resonances were then systematically analyzed in 1990s.[10] In the literature, RWGs have been called in many different ways: guided-mode resonances,[10] leaky-mode resonances,[11] and corrugated waveguides.[12] All these terms express the main physical property of these structures: the diffracted wave from the grating is transferred as coupled mode in the waveguide material where it efficiently interacts with the incoming wave in a leaky process, and it is finally out-coupled.

Subwavelength RWGs with single periodicity cannot usually be applied for beam steering, because the beam deflection happens only at the zeroth order (either in transmission or reflection).[13] We use the term beam steering to indicate a passive beam steering,[14,15] where the radiation pattern is not actively controlled (i.e., mechanically or electronically). However, RWGs made with two adjacent gratings having different finite number of periods can be engineered to create a functional beam steering element, as reported in an earlier work,[5] where the light from

*Address all correspondence to: Benjamin Gallinet, E-mail: benjamin.gallinet@csem.ch

1934-2608/2018/$25.00

a point source is filtered and constructively redirected to another point. However, large-scale patterns are time-demanding to design because of the many degrees of freedom of the system, i.e., the orientation and the period of the two gratings of each element, the waveguide thickness, and the position of each element to preserve the phase matching with the adjacent ones at the observation point.

Here, we propose a design method that allows creating large-scale patterns of RWG elements with a technique based on positioning the beam steering elements along confocal prolate spheroid arrangements. This approach can be applied to any metasurface structure. Because of the intrinsic properties of the quadric curves, the phase matching of the designed patterns is very robust against fabrication tolerances.[16]

As a demonstration of practical implementation, we fabricate a designed pattern with an electron beam lithography optimized for large areas, and with a nanoimprint embossing replication on a thin PMMA foil, coated with thin-film ZnS and laminated into a business card.

2 Analytical Models

We first describe the properties of a passive beam steering element made with two adjacent RWGs. Then, we show how to use the element to design a large pattern by varying the periods, the orientation, and the position of each element, using as a design rule a system of confocal prolate spheroids.

2.1 *Properties of the Beam Steering Element Made with Two Resonant Waveguide Gratings*

The passive beam steering element used in this work consists of two adjacent RWGs having different finite numbers of periods but sharing the same substrate and the same coated waveguide material.[5] A schematic is shown in Fig. 1, where a white broadband light source coming at a specific orientation (θ_{in}, ϕ_{in}) is filtered by the first RWG (with period Λ_1) and coupled into the corrugated waveguide. Here, the central in-coupled wavelength is λ. Part of the coupled mode is released by the same RWG, due to its intrinsic leaky behavior. Because of impedance matching, part of the coupled mode reaches the second RWG (with period Λ_2) and resonates again, coupling the energy out from the RWG plane. The beam from the second RWG is out-coupled and reflected at another orientation in space $(\theta_{out}, \phi_{out})$. Because of the symmetry of the structure in the z-direction, part of the beam is also out-coupled in transmission $(-\theta_{out}, \phi_{out})$.

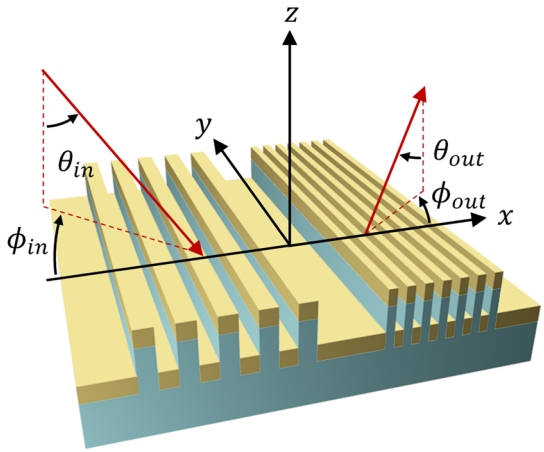

Fig. 1 Beam steering element used to filter and redirect a specific spectral of light coming at a specific orientation (θ_{in}, ϕ_{in}) on the first RWG (with period Λ_1) at another orientation $(\theta_{out}, \phi_{out})$ from the second RWG (with period Λ_2).

The unit cell can work in both in-plane regime (i.e., when the incoming light is oriented perpendicular to the grating lines) and in fully conical regime (i.e., when the incoming light is parallel to the grating lines), as well as in any intermediate position.

2.2 *System of Confocal Prolate Spheroids*

A large pattern of these passive beam steering elements can be created to filter a specific spectral portion of a point source and to redirect and focus it to another point in the space, viz. the observation point, by positioning the beam steering elements on a surface with different grating periods and orientation. Moreover, the arrangements of these elements must preserve the phase coherence of the whole pattern at the observation point.

Here, we report a design technique that allows rapid creation of the pattern. This technique is based on geometrical and ray-tracing considerations of prolate spheroid mirrors, which reflect any ray of light coming from one focal point (f_s) to the other focal point (f_p). All the light rays preserve the phase coherence when reaching the second focal point, since by geometry their paths have the same length. For a pattern covering a given surface, confocal spheroids with different radii are used. The difference in optical path length among rays reflected from the different spheroids must be a multiple of the wavelength to ensure constructive interference at the observation point.

Following these geometrical considerations, we choose a prolate spheroid Q having the foci and the semimajor axis a on the x-axis, and the semiminor axis b lying on the y- and z-axes [Fig. 2(a)]. We place the source point f_s and the observation point f_o in the position of the two foci of Q such that the surface with the pattern of beam steering elements (defined as Σ) is intersected by such a spheroid Q. For the purpose of this work, we assume that the surface

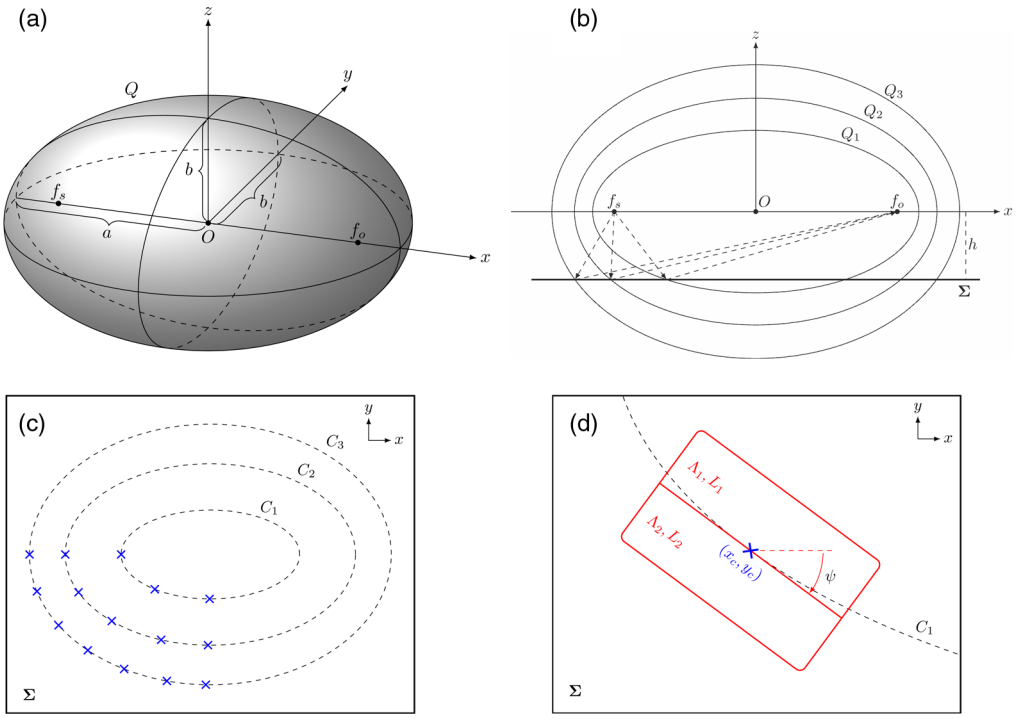

Fig. 2 Scheme of the design method based on confocal prolate spheroid arrangements. (a) A prolate spheroid Q. (b) Section of three confocal prolate spheroid, where the structured surface Σ is used to filter and steer the light from a point source set in the focal point f_s to an observation point set in the focal point f_o. (c) Beam steering elements (marked as blue ticks) are placed on the plane Σ and are arranged on sections of the confocal prolate spheroids intersecting the plane Σ. (d) A beam steering element (rounded red rectangle) made with two RWGs, where one RWG (Λ_1, L_1) is responsible to in-couple and filter the light coming from f_s and the other RWG (Λ_2, L_2) is used to out-couple the light to f_o.

Σ is planar and normal to the z-axis. Moreover, we consider the case where the source point f_s and the observation point f_o have the same distance h to that surface so that a spheroid described by the two foci (f_s, f_o) has its semimajor axis parallel to the surface Σ. However, the proposed design rules are valid even in the case when the source and observation points are not parallel to the x-axis or when the surface Σ is not planar. If the foci (f_s, f_o) are not parallel to the x-axis it is still possible to use this system and apply transformation matrices for any rotation or translation, which is well known in Euclidean geometry.

We set the origin of the reference system in the middle between the two foci, and we define the half distance between the two foci as f

$$f = \frac{1}{2}\overline{f_s f_o} = \sqrt{a^2 - b^2}, \tag{1}$$

where a and b are, respectively, the major- and minor-axes of the prolate spheroid Q. Such prolate spheroid can be, therefore, defined as

$$Q: \ \frac{x^2}{a^2} + \frac{y^2 + z^2}{b^2} = 1. \tag{2}$$

Since $h < b$ (i.e., the plane Σ intersects the prolate spheroid), the intersection of the spheroid with such a plane Σ defines an ellipse C lying on Σ

$$C: \ \frac{x^2}{a^2 \cdot \left(1 - \frac{h^2}{a^2 - f^2}\right)} + \frac{y^2}{a^2 - f^2 - h^2} = 1. \tag{3}$$

If a beam steering element [Fig. 2(d)] is placed on the planar surface Σ with its center (x_c, y_c) on the ellipse defined in Eq. (1) and oriented by an angle ψ such that the grating lines are parallel to the tangent of the ellipse in (x_c, y_c), it is then possible to numerically compute the period of the two gratings such that a broadband light beam coming from f_s is filtered to the desired portion of spectrum and redirected to f_o. If multiple beam steering elements have their centers on the ellipse C of Eq. (1), the path distances from f_s to f_o will all have the same length, because of the geometrical considerations about prolate spheroids described before [Fig. 2(c)]. Moreover, the out-coupled beams have the same phase difference from the in-coupled beams, since the optical paths and phases gained during the propagation in the RWG having the same length are constant.[17] All the light beams have, therefore, the same phase at the observation point f_o.

To design a full pattern that covers the surface Σ, a number of n prolate spheroids (Q_n) with different radii and intersecting Σ have to be used. Since all those spheroids share the same foci (f_s, f_o), they are described by the geometrical formalism of confocal prolate spheroids [Fig. 2(b)]

$$Q_n: \ \frac{x^2}{(a+k)^2} + \frac{y^2 + z^2}{(a+k)^2 - f^2} = 1, \tag{4}$$

where k is a constant used to increase the length of the semimajor axis.

The intersection of such a family of confocal prolate spheroids Q_n with the plane Σ is described by a family of n nonconfocal ellipses

$$C_n: \ \frac{x^2}{(a+k)^2 \cdot \left[1 - \frac{h^2}{(a+k)^2 - f^2}\right]} + \frac{y^2}{(a+k)^2 - f^2 - h^2} = 1, \tag{5}$$

where the first and the second denominators denote the squares of the semimajor and semiminor axes of the ellipses.

The constant k defines the distance between the different spheroids or ellipses and must be chosen carefully to preserve the phase coherence of the beam-redirecting elements among the different ellipses. In particular, to have constructive phase interference for the whole pattern at the observation point f_o, the path length between the source and the observer must be a multiple of the redirected central wavelength λ.

3 Design and Fabrication

The design method described in Sec. 2 enables the creation of a beam steering device that can be used in a variety of fields. In this paper, we show the implementation for an optical security device, where we design and fabricate three transparent structures that show uniform colors (i.e., red, green, and blue) only using a standard smartphone located in a specific spatial position on top of them.

3.1 *Computation of the Pattern*

For each realization, we engineered a flat surface of 1×1 cm^2 composed by >20.000 passive beam steering elements, where the light coming from the flash of the smartphone is spectrally filtered and in-coupled in one RWG. The other RWG of the unit cell is responsible to out-couple the guided-mode toward the camera of the smartphone. Moreover, all the beam steering elements have been designed to create constructive interference of all the out-coupled beams in the position of the camera and the smartphone, where they are focused. The system is in off-axis configuration because the angle between the source point f_s (i.e., the flash) and the observer f_o (i.e., the camera) is nonzero but is determined by the system of confocal prolate spheroids described in Sec. 2. Moreover, the beam steering elements work in conical illumination,[18] because the grating grooves are not necessarily perpendicular to the incoming light. In Fig. 3, the engineered values of the grating periods (Λ_1 and Λ_2) and the orientation of the beam steering elements with respect to the x-axis are reported for the label responsible to redirect red light. Further details of the realizations of this label are reported on Quaranta et al.[5]

3.2 *Fabrication with Prefracturing Techniques*

First, the fabrication of the designed pattern involves the electron beam lithography process. Note that in Fig. 3, the range of the grating periods is relatively broad (i.e., between 280 and 440 nm), as well as the possible grating orientations (i.e., from 20 deg to 60 deg). Due

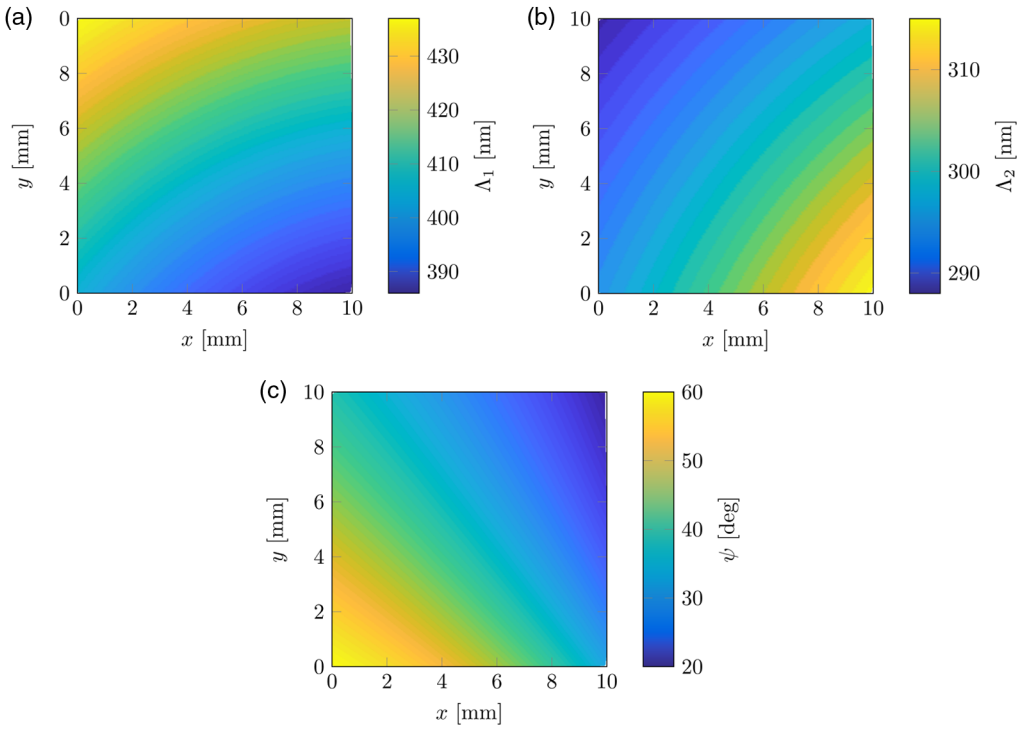

Fig. 3 Engineered label with the proposed design method that shows a uniform red color on the screen of a smartphone when shone with its flash in a specific spectral position. Values of (a) Λ_1, (b) Λ_2, and (c) ψ are shown [Fig. 2(d)].

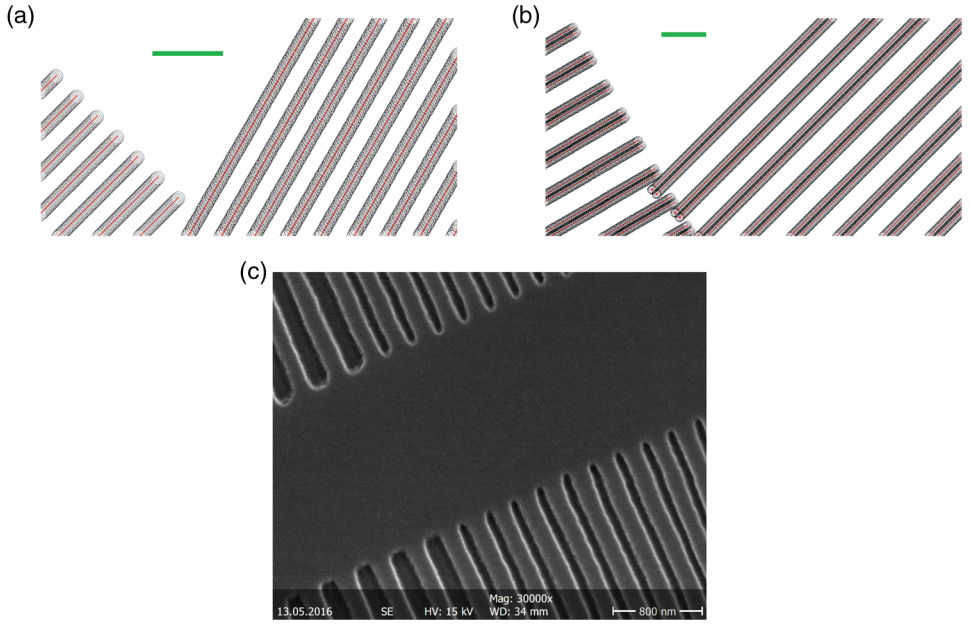

Fig. 4 Sections of prefractured patterns in the cases of (a) one and (b) two stripes configurations. The exposure positions with the predicted beam diameter are also shown. The green scale bar is 500 nm. (c) SEM image of different gratings.

to the large diversity of shapes, the standard approach used to create the structure by electron beam lithography is to use a small electron beam with low current (e.g., a 10-nA beam). However, the use of small beams requires longer exposure times compared with the use of larger beams, and this issue can be a limiting factor to up-scale the size of beam steering patterns designed with the proposed method. Therefore, we implemented a custom prefracturing of the designed pattern such that it could be exposed with a larger electron beam (i.e., with 200-nA beam).

In the prefracturing process, we split each grating line into one or more smaller stripes, depending on the size of the grating period. Each stripe width is equal to the beam step size used in the fracturing. The beam step size used is, therefore, smaller than the beam diameter: for the purpose of this work we used a beam step size of 10 nm and a beam diameter of about 100 nm. In this way, it is possible to expose the pattern with a large electron beam but preserving enough accuracy to expose a large variety of grating periods and grating orientations. Figures 4(a) and 4(b) show two prefractured gratings with one and two stripes. We used the electron beam EBPG5000ES to expose HSQ photoresist (HSQ XR1541 004) on a Si wafer.

The master wafer was then replicated on a Ni-shim. Subsequently, a replica of the structure was made by hot-embossing nanoimprint lithography on a thin PMMA foil. Afterward, the waveguiding layer of ZnS was added with PVD and the structure was finally encapsulated and glued on a business card. A picture of the business card with the hidden label is shown in Fig. 5(a).

3.3 *Experimental Observation and Characterization of the Transparency*

To test the realization, a smartphone (i.e., Asus Zenfone 2) was fixed on a stand at 6.5 cm above the business card, with the flash, and the camera centered in the chosen positions of source (f_s) and observer (f_o), respectively. In this configuration, the light of the flash is filtered and redirected to the camera, showing colorful squares [Fig. 5(b)]. It is possible to observe the same colors with negligible difference even when tested with other smartphones, such as Nokia Lumia 920, or iPhone 6s. Thanks to RWGs, the optical effect has been shown to work with a low coherent light source, such as the white LED of the smartphone. However, it is also possible to use light sources with higher coherence. The pattern is almost invisible by naked eye, and it has small diffraction noise. It is possible to observe defects related to the fabrication on PMMA

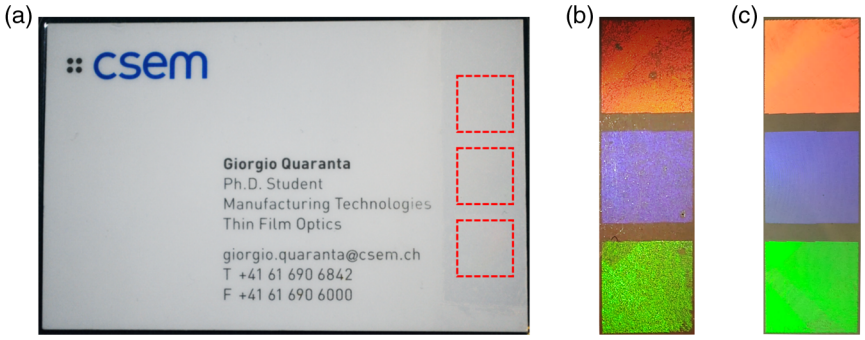

Fig. 5 Figures of the final device, embedded on a business card. (a) Business card with the structured patterns highlighted with dashed squares, (b) pattern revealed on a smartphone when it is placed in the proper position and the flash is turned on, and (c) alternative fabrication on glass substrate.

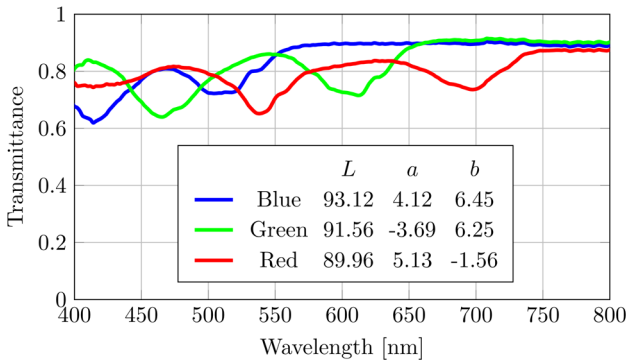

Fig. 6 Transmittance at normal incidence from the three squared patterns, normalized to the illumination in air, showing the high transparency of the patterns. The inset reports the computed Lab colors of these spectra, using the CIE Standard Illuminant D65 and the CIE 1964 Color Space.

with hot-embossing technique. These defects are not present in the same device created on a glass substrate [Fig. 5(c)]. Some defects and inhomogeneities are left visible on the glass sample due to electron beam exposure approximations, which can be easily addressed.

To quantitatively characterize the high transparency of the sample in environmental illumination, we measured the transmittance with a spectrometer (Spectrascan PR-730, Photo Research) normalized to the illumination in air. The light source used was generated from a halogen lamp (HL-2000, Ocean Optics) and collimated with a parabolic reflective collimator (RC04SMA, Thorlabs) perpendicularly to each of the three squared patterns. The results are reported in Fig. 6, as well as the computed Lab colors of such spectra using the CIE Standard Illuminant D65 and the CIE 1964 Color Space. We can observe a general high transparency level of all the three structures, with high values of the coordinate L. Furthermore, we can notice the presence of two dips for each measurement, related to the resonances of the RWGs in transmission at normal incidence for both Λ_1 and Λ_2. Due to those dips, the coordinates a and b are different than zero and thus slightly different from true gray neutrality.

4 Summary and Outlook

In summary, we have presented and explained a design method to efficiently and robustly create focusing patterns of passive beam steering elements whose arrangement is based on the geometrical model of confocal prolate spheroids, where the foci are set in the position of the source point and observer point. As it is based only on ray tracing and wavefront phase engineering considerations, this method can be applied to any kind of metasurface redirecting elements.

Conversely to the complex mastering process, the fabrication process of these devices is up-scalable since it can be reproduced with roll-to-roll nanoimprint lithography and PVD coating. All three primary colors can be combined in a device using a common waveguiding layer. This requirement is needed for applications where high throughput is needed, i.e., for optical security. The pattern is also highly transparent when seen by naked eye; therefore, it can be implemented as a noninvasive anticounterfeiting label. Because of its transparency and configuration, such a structure can be combined with other optical security devices, increasing their robustness to counterfeiters. Finally, the authentication procedure could be digitally automated and not user controlled.

The proposed methodology can be applied to realize passive beam steering structures for a variety of other fields. When one focal point is set to infinity, multifocal (i.e., different colors focused in designed positions), or monochromatic lenses can be designed with a system of confocal paraboloids. This method could also be implemented in gas sensing, where a pattern appears on the smartphone only when no gas is detected. This behavior can be realized with refractive-index sensing[19] or absorption sensing.[3] Furthermore, see-through optical combiners for near-eye displays could be designed by redirecting the light from a microprojector (in the position of the point source f_s) to the human eye (in the position of the observer f_o).

References

1. D. Rosenblatt, A. Sharon, and A. A. Friesem, "Resonant grating waveguide structures," *IEEE J. Quantum Electron.* **33**(11), 2038–2059 (1997).
2. S. Tibuleac and R. Magnusson, "Reflection and transmission guided-mode resonance filters," *J. Opt. Soc. Am. A* **14**(7), 1617–1626 (1997).
3. L. Davoine et al., "Resonant absorption of a chemically sensitive layer based on waveguide gratings," *Appl. Opt.* **52**(3), 340–349 (2013).
4. T. Khaleque, *Guided-Mode Resonant Solar Cells and Flat-Top Reflectors: Analysis, Design, Fabrication and Characterization*, University of Texas, Arlington (2014).
5. G. Quaranta et al., "Color-selective and versatile light steering with up-scalable subwavelength planar optics," *ACS Photonics* **4**(5), 1060–1066 (2017).
6. H. Li et al., "High-performance binary blazed grating coupler used in silicon-based hybrid photodetector integration," *Opt. Eng.* **53**(9), 097106 (2014).
7. H. Li et al., "Highly efficient polarization-independent grating coupler used in silica-based hybrid photodetector integration," *Opt. Eng.* **53**(5), 057105 (2014).
8. R. W. Wood, "On a remarkable case of uneven distribution of light in a diffraction grating spectrum," *Proc. Phys. Soc. London* **18**(1), 269–275 (1902).
9. A. Hessel and A. A. Oliner, "A new theory of Wood's anomalies on optical gratings," *Appl. Opt.* **4**(10), 1275–1297 (1965).
10. S. S. Wang et al., "Guided-mode resonances in planar dielectric-layer diffraction gratings," *J. Opt. Soc. Am. A* **7**(8), 1470–1474 (1990).
11. M. Shokooh-Saremi and R. Magnusson, "Wideband leaky-mode resonance reflectors: influence of grating profile and sublayers," *Opt. Express* **16**(22), 18249–18263 (2008).
12. P. Vincent and M. Nevière, "Corrugated dielectric waveguides: a numerical study of the second-order stop bands," *Appl. Phys.* **20**(4), 345–351 (1979).
13. I. Avrutsky and R. Rabady, "Waveguide grating mirror for large-area semiconductor lasers," *Opt. Lett.* **26**(13), 989–991 (2001).
14. F. Koyama and X. Gu, "Beam steering, beam shaping, and intensity modulation based on VCSEL photonics," *IEEE J. Sel. Top. Quantum Electron.* **19**(4), 1701510 (2013).
15. C. W. Oh et al., "Free-space transmission with passive 2D beam steering for multi-gigabit-per-second per-beam indoor optical wireless networks," *Opt. Express* **24**(17), 19211–19227 (2016).
16. Y. Bao et al., "Enhanced optical performance of multifocal metalens with conic shapes," *Light* **6**, e17071 (2017).
17. P. K. Sahoo, S. Sarkar, and J. Joseph, "High sensitivity guided-mode-resonance optical sensor employing phase detection," *Sci. Rep.* **7**(1), 7607 (2017).

18. C. A. Palmer and E. G. Loewen, *Diffraction Grating Handbook*, Newport Corporation Springfield, Ohio (2005).
19. K. Schmitt and C. Hoffmann, "High-refractive-index waveguide platforms for chemical and biosensing," in *Optical Guided-Wave Chemical and Biosensors I*, M. Zourob and A. Lakhtakia, Eds., Vol. **7**, pp. 21–54, Springer, Berlin, Heidelberg (2010).

Biographies for the authors are not available.